

A parametric study on the thermal performance of cross-corrugated solar air collectors

Wenxian Lin ^{a,b,*}, Wenfeng Gao ^a, Tao Liu ^a

^a Solar Energy Research Institute, Yunnan Normal University, Kunming 650092, PR China

^b School of Engineering, James Cook University, Townsville, QLD 4811, Australia

Received 27 April 2005; accepted 10 October 2005

Abstract

A comprehensive parametric study has been carried out in this paper on the thermal performance of cross-corrugated solar air collectors. These collectors consists of a wavelike absorbing plate and a wavelike bottom plate which are crosswise positioned to form the air flow channel. Two types of these collectors are considered. For the Type 1 collector, the wavelike shape of the absorbing plate is along the flow direction and that of the bottom plate is perpendicular to the flow direction, while for the Type 2 collector it is the wavelike shape of the bottom plate that is along the flow direction and that of the absorbing plate is perpendicular to the flow direction. The aim of the use of the cross-corrugated absorbing plate and bottom plate is to enhance the turbulence and the heat transfer rate inside the air flow channel which are crucial to the improvement of efficiencies of solar air collectors. To quantify the achievable improvements with the cross-corrugated absorbing and bottom plates, a flat-plate solar air collector which has both a flat absorbing plate and a flat bottom plate, is also considered. The thermal performance of these three types of solar air collector are analyzed and compared under various configurations and operating conditions. The results show that although the thermal performance of the Type 2 collector is just slightly superior to that of the Type 1 collector both of these cross-corrugated solar air collectors have a significantly superior thermal performance to that of the flat-plate one. It is also found that to achieve a higher collector efficiency, it is essential to construct the collectors having slender configurations along the air flow direction, to maintain a small mean gap between the absorbing plate and bottom plate, to use selected coatings on the absorbing plate and glass cover, to maintain a higher air mass flow rate, and to operate the collectors with the inlet fluid temperature close to that of the ambient fluid. © 2005 Elsevier Ltd. All rights reserved.

Keywords: Cross-corrugated solar air heater; Thermal performance; Heat transfer; Wavelike absorbing plate; Wavelike bottom plate

1. Introduction

Solar air collectors are key components in many engineering applications, such as in building heating systems, in solar drying devices, etc. [1,2]. Due to the poor thermal conductivity and small heat capacity of air, the convective heat transfer rate inside the air flow

channel where the air is heated is low, and a great deal of effort has been made to increase this rate [3]. One of the effective ways to augment the convective heat transfer rate in channel flows is to increase the heat transfer surface area and to increase turbulence inside the channel by using fins or corrugated surfaces [4,5] and many studies have been carried out on this topic. For example, the convective heat transfer in a Vee-trough linear solar collector was studied by Meyer et al. [6] while the natural convection in a channel formed by a Vee-shaped surface and a flat plate was studied numerically and experimentally by Zhao and

* Corresponding author. Address: Solar Energy Research Institute, Yunnan Normal University, Kunming 650092, PR China. Tel.: +86 871 5516299; fax: +86 871 5516217.

E-mail address: linwenxian@ynnu.edu.cn (W. Lin).

Li [7]. Stasiek [8] carried out experimental studies on the heat transfer and fluid flow across corrugated-undulated heat exchanger surfaces. Piao et al. [10,9] investigated experimentally natural, forced and mixed convective heat transfer in a cross-corrugated channel solar air heater. Noorshahi, Hall and Glakpe [11] conducted a numerical study on the natural convection in a corrugated enclosure with mixed boundary conditions. Gao et al. [12,13] numerically simulated the natural convection inside the channel formed by a flat cover and a wavelike absorbing plate.

In this paper, a detailed parametric study has been carried out to investigate the thermal performance of cross-corrugated solar air collectors in which the wavelike shapes of the absorbing plate and the bottom plate are perpendicular to each other and the air flows through the channel formed by these two plates. Comparisons have also been made to that of a flat-plate solar air collector to show the efficiency improvement achievable with the use of the cross-corrugated absorbing plate and bottom plate.

2. Theoretical analysis

Two types of cross-corrugated solar air collectors are considered in this paper. Both types consist of a single flat glass cover, a wavelike absorbing plate and a wavelike bottom plate which is attached by a back insulation beneath. The channel formed by the absorbing plate and the bottom plate is the air flow channel where the air is heated by the absorbed solar radiation on the absorbing plate. In the Type 1 collector, the wavelike shape of the absorbing plate is along the air flow direction and that of the bottom plate is perpendicular to the air flow direction. In the Type 2 collector, however, it is the wavelike shape of the bottom plate that is along the air flow direction and that of the absorbing plate is perpendicular to the flow direction. The aim of the use of the cross-corrugated absorbing plate and bottom plate, as mentioned above, is to enhance the turbulence and the heat transfer rate inside the air flow channel which are crucial to the improvement of efficiencies of solar air collectors. To quantify the achievable improvements with the cross-corrugated absorbing and bottom plates, a flat-plate solar air collector (referred to as the Type 3 collector), which has both a flat absorbing plate and a flat bottom plate, is also analyzed.

To model the collectors considered, a number of simplifying assumptions can be made to lay the foundations without obscuring the basic physical situation.

These assumptions are as follows:

1. Thermal performance of collectors is steady state.
2. There is a negligible temperature drop through the glass cover, the absorber plate and the bottom plate.

3. There is one-dimensional heat flow through the back insulation which is in the direction perpendicular to the air flow.
4. The sky can be considered as a blackbody for long-wavelength radiation at an equivalent sky temperature.
5. Loss through front and back are to the same ambient temperature.
6. Dust and dirt on the collector and the shading of the collector absorbing plate are negligible.
7. Thermal inertia of collector components is negligible.
8. Operating temperatures of collector components and mean air temperatures in air channels are all assumed to be uniform.
9. Temperature of the air varies only in the flow direction.
10. All air channels are assumed to be free of leakage.
11. Thermal losses through the collector backs are mainly due to the conduction across the insulation and those caused by the wind and the thermal radiation of the insulation are assumed negligible.

2.1. Energy balance equations

If the solar insolation rate incident on the glass cover is I (W/m^2), the transmissivity of solar radiation of the glass cover is τ_c , and the absorptivity of solar radiation of the absorbing plate is α_{ap} , the solar radiation absorbed by the absorbing plate per unit area, S (W/m^2), which is equal to the difference between the incident solar radiation and the optical loss, is as follows [1]

$$S \simeq 0.97\tau_c\alpha_{ap}I. \quad (1)$$

This absorbed energy S is distributed to thermal losses through the glass cover and the bottom and to useful energy gain q_u (W/m^2) which heats the air in the channel from the inlet temperature T_{fi} (K) to the outlet temperature T_{fo} (K), resulting in the mean air temperature $T_f = (T_{fi} + T_{fo})/2$.

On the glass cover, the energy gains are $\alpha_c I$, the absorbed solar radiation by the cover where α_c is the absorptivity of solar radiation of the glass cover, the heat transferred by natural convection from the absorbing plate represented by $h_{c,ap-c}$ ($\text{W}/\text{m}^2 \text{K}$) which is the convection heat transfer coefficient between the cover and the absorbing plate, and that transferred by thermal radiation from the absorbing plate represented by $h_{r,ap-c}$ ($\text{W}/\text{m}^2 \text{K}$) which is the radiation heat transfer coefficient between the cover and the absorbing plate. The energy loss through the glass cover are the heat transferred by the convection due to wind represented by h_w ($\text{W}/\text{m}^2 \text{K}$) which is the wind convection heat transfer coefficient, and that transferred by the thermal radiation from the cover to the sky at T_s (K) represented

by $h_{r,c-s}$ ($\text{W/m}^2 \text{K}$) which is the radiation heat transfer coefficient between the cover and the sky. Hence, the energy balance in the glass cover requires

$$\begin{aligned} \alpha_c I + (h_{c,ap-c} + h_{r,ap-c})(T_{ap} - T_c) \\ = (h_w + h_{r,c-s})(T_c - T_a), \end{aligned} \quad (2)$$

where T_{ap} (K) and T_c (K) are the mean temperature on the absorbing plate and on the glass cover, and T_a (K) is the ambient temperature.

On the absorbing plate, the absorbed solar radiation S is distributed to thermal losses to the glass cover by natural convection represented by $h_{c,ap-c}$ and by thermal radiation represented by $h_{r,ap-c}$, to the bottom plate by thermal radiation represented by $h_{r,ap-bp}$ which is the radiation heat transfer coefficient between the absorbing plate and the bottom plate, and to the fluid by convection represented by $h_{c,ap-f}$ ($\text{W/m}^2 \text{K}$) which is the convection heat transfer coefficient of fluid on the absorbing plate. Hence the energy balance on the absorbing plate requires

$$\begin{aligned} S = (h_{c,ap-c} + h_{r,ap-c})(T_{ap} - T_c) + h_{r,ap-bp}(T_{ap} - T_{bp}) \\ + h_{c,ap-f}(T_{ap} - T_f), \end{aligned} \quad (3)$$

where T_{bp} (K) is the mean temperature on the bottom plate.

For the fluid, the heat gained from the absorbing plate by convection represented by $h_{c,ap-f}$ is distributed to the heat gain q_u which is carried away by the fluid and the thermal loss to the bottom plate by convection represented by $h_{c,f-ap}$ ($\text{W/m}^2 \text{K}$) which is the convection heat transfer coefficient of fluid on the bottom plate, resulting in the following energy balance,

$$h_{c,ap-f}(T_{ap} - T_f) = q_u + h_{c,f-ap}(T_f - T_{bp}), \quad (4)$$

where $q_u = c_p \dot{m}_f (T_{fo} - T_{fi})$, in which c_p (J/kg K) is the specific heat of air and \dot{m}_f ($\text{kg/m}^2 \text{s}$) is the air mass flow rate per unit area of collector.

On the bottom plate, the heat gains from the fluid via convection represented by $h_{c,f-ap}$ and from the absorbing plate via thermal radiation represented by $h_{r,ap-bp}$ are balanced by the thermal loss to the ambient via conduction represented by h_b ($\text{W/m}^2 \text{K}$) which is the conduction heat transfer coefficient across the insulation, that is,

$$\begin{aligned} h_{r,ap-bp}(T_{ap} - T_{bp}) + h_{c,f-ap}(T_f - T_{bp}) \\ = h_b(T_{bp} - T_a). \end{aligned} \quad (5)$$

With the assumption of $T_f = (T_{fo} + T_{fi})/2$, it is found from Eq. (2) that

$$T_c = \frac{\alpha_c I + (h_{c,ap-c} + h_{r,ap-c})T_{ap} + (h_w + h_{r,c-s})T_a}{h_{c,ap-c} + h_{r,ap-c} + h_w + h_{r,c-s}}, \quad (6)$$

from Eq. (3)

$$T_{ap} = \frac{S + (h_{c,ap-c} + h_{r,ap-c})T_c + h_{r,ap-bp}T_{bp} + h_{c,ap-f}T_f}{h_{c,ap-c} + h_{r,ap-c} + h_{r,ap-bp} + h_{c,ap-f}}, \quad (7)$$

from Eq. (4)

$$T_f = \frac{h_{c,ap-f}(T_{ap} + T_{bp}) + 2c_p \dot{m}_f T_{fi}}{2h_{c,ap-f} + 2c_p \dot{m}_f}, \quad (8)$$

and from Eq. (5)

$$T_{bp} = \frac{h_b T_a + h_{r,ap-bp}T_{ap} + h_{c,ap-f}T_f}{h_b + h_{r,ap-bp} + h_{c,ap-f}}. \quad (9)$$

The instantaneous efficiency of solar heat gain of the collector is

$$\eta = \frac{q_u}{I} = \frac{c_p \dot{m}_f (T_{fo} - T_{fi})}{I} = \frac{2c_p \dot{m}_f (T_f - T_{fi})}{I}. \quad (10)$$

2.2. Determination of heat transfer coefficients

The convection heat transfer coefficient from the glass cover due to wind is recommended by McAdams [14] as

$$h_w = 5.7 + 3.8V_w, \quad (11)$$

where V_w (m/s) is the wind velocity of the ambient air and it is usually assumed that $V_w = 1.5$ m/s [15], which gives $h_w = 11.4$ $\text{W/m}^2 \text{K}$. In this paper, $h_w = 11.4$ $\text{W/m}^2 \text{K}$ is also used.

The radiation heat transfer coefficient from the glass cover to sky referred to the ambient air temperature T_a (K) may be obtained as follows [15]

$$h_{r,c-s} = \sigma \epsilon_c (T_c + T_s)(T_c^2 + T_s^2) \frac{(T_c - T_s)}{(T_c - T_a)}, \quad (12)$$

where $\sigma = 5.57 \times 10^{-8}$ $\text{W/m}^2 \text{K}^4$ is the Stefan–Boltzmann constant, ϵ_c is the emissivity of thermal radiation of the glass cover, and the sky temperature T_s (K) is estimated by the formulation given by Swinbank [16]

$$T_s = 0.0552T_a^{1.5}. \quad (13)$$

The radiation heat transfer coefficients between the glass cover and the absorbing plate and between the absorbing plate and the bottom plate are predicted, respectively, by

$$h_{r,ap-c} = \frac{\sigma(T_{ap}^2 + T_c^2)(T_{ap} + T_c)}{1/\epsilon_{ap} + 1/\epsilon_c - 1}, \quad (14)$$

and

$$h_{r,ap-bp} = \frac{\sigma(T_{ap}^2 + T_{bp}^2)(T_{ap} + T_{bp})}{1/\epsilon_{ap} + 1/\epsilon_{bp} - 1}, \quad (15)$$

where ϵ_{ap} and ϵ_{bp} are the emissivities of thermal radiation of the absorbing plate and the bottom plate.

The conduction heat transfer coefficient across the insulation is estimated by

$$h_b = \frac{k_i}{\Delta_i}, \quad (16)$$

where k_i (W/m K) is the thermal conductivity of the insulation and Δ_i (m) is the mean thickness of the insulation.

The convection heat transfer coefficient between the glass cover and the absorbing plate is calculated by

$$h_{c,ap-c} = Nu_{ap-c} \frac{k}{H_c}, \quad (17)$$

where k (W/m K) is the thermal conductivity of air, H_c is the mean gap thickness between the cover and the absorbing plate, and Nu_{ap-c} is the Nusselt number for the natural convection in the channel formed by the cover and the absorbing plate.

For the Type 1 collector, the following correlation developed by Zhao and Li [7] can be used to approximate Nu_{ap-c}

$$Nu_{ap-c} = 0.1673(Ra \cos \theta)^{0.2917}, \quad (18)$$

where θ ($^\circ$) is the angle of inclination of the collector and Ra is the Rayleigh number which is defined as

$$Ra = \frac{\rho^2 c_p g \beta (T_{ap} - T_c) H_c^3}{k \mu}, \quad (19)$$

in which ρ (kg/m³), β (1/K) and μ (kg/m s) are the density, thermal expansion coefficient and dynamic viscosity of air, and g (m/s²) is the gravitational constant.

For the Type 2 and Type 3 collectors, Nu_{ap-c} can be estimated by the following correlation [17]

$$Nu_{ap-c} = 1 + 1.44 \left[1 - \frac{1708(\sin 1.8\theta)^{1.6}}{Ra \cos \theta} \right] \left[1 - \frac{1708}{Ra \cos \theta} \right]^+ + \left[\left(\frac{Ra \cos \theta}{5830} \right)^{1/3} - 1 \right]^+, \quad (20)$$

where the “+” symbol in the superscript means that only positive values of the terms in the square brackets are to be used (i.e., use zero if the term is negative). This correlation is valid for $0^\circ \leq \theta \leq 75^\circ$.

The convection heat transfer coefficients for the fluid moving on the absorbing plate and on the bottom plate, are calculated by

$$h_{c,ap-f} = h_{c,f-bp} = Nu_{ap-f} \frac{k}{D_h}, \quad (21)$$

where $D_h = 2WH_g/(W + H_g)$ (m) is the hydraulic diameter of the air flow channel formed by the absorbing plate and the bottom plate, W (m) is the collector width, H_g (m) is the mean gap thickness between the absorbing plate and the bottom plate, and Nu_{ap-f} is the Nusselt number for the convection of fluid moving in the air flow channel.

For the Type 1 and Type 2 collectors, Nu_{ap-f} can be estimated by the following correlation [9,10]

$$Nu_{ap-f} = 0.0743Re^{0.76}, \quad (22)$$

where Re is the Reynolds number defined as follows,

$$Re = \frac{\rho \bar{U}_f D_h}{\mu}, \quad (23)$$

in which \bar{U}_f (m/s) is the mean velocity of fluid in the channel. This correlation is valid for $3000 \leq Re \leq 50000$.

For the Type 3 collector, however, Nu_{ap-f} is estimated by the following correlation [18]

$$Nu_{ap-f} = 0.0158Re^{0.8}, \quad (24)$$

where Re is the Reynolds number defined as follows,

$$Re = \frac{2\rho \bar{U}_f H_g}{\mu}, \quad (25)$$

which is for full developed turbulent flow in the channel.

When the air temperature T (K) is in the range of 280–470 K, the following empirical correlations can be obtained from [19] to estimate the density, thermal conductivity and dynamic viscosity of air,

$$\rho = 3.9147 - 0.016082T + 2.9013 \times 10^{-5}T^2 - 1.9407 \times 10^{-8}T^3, \quad (26)$$

$$k = (0.0015215 + 0.097459T - 3.3322 \times 10^{-5}T^2) \times 10^{-3}, \quad (27)$$

$$\mu = (1.6157 + 0.06523T - 3.0297 \times 10^{-5}T^2) \times 10^{-6}, \quad (28)$$

while constant $\beta = 1/T$ (1/K) and $c_p \simeq 1000$ J/kg K can also be assumed.

2.3. Solutions of temperatures and efficiency

It is apparent from Eqs. (6)–(10) that no analytic solutions can be obtained for the temperatures T_c , T_{ap} , T_{bp} , and T_f and the efficiency η as most of the heat transfer coefficients are functions of these temperatures. Hence, the values of these parameters will be obtained numerically with an iteration method. The procedure is first using guessed temperatures to calculate the heat transfer coefficients, which are then used to estimate new temperatures, and if all these new temperatures are larger than 0.01% from their respective guessed values then these new temperatures will be used as the guessed temperatures for the next iteration and the process will be repeated until all the newest temperatures obtained are within $\pm 0.01\%$ from their respective previous values.

3. Results and discussion

The configuration parameters for the solar air collectors considered here are W , L , H_g , H_c , Δ_i , k_i , ϵ_{ap} , ϵ_{bp} , ϵ_c ,

α_{ap} , α_c , and τ_c , and the parameters featuring the operating conditions are I , θ , \dot{m}_f , and T_{fi} , respectively.

The parameters characterizing the thermal performance of these collectors are η , T_c , T_{ap} , T_{bp} , $\Delta T_f = T_{fo} - T_{fi}$ which is the fluid temperature difference at the inlet and the outlet, $h_{c,ap-f}$, $h_{c,ap-c}$, $h_{r,ap-bp}$, $h_{r,ap-c}$, and $h_{r,c-s}$, respectively.

In this section, solutions are first obtained under the typical configurations and operating conditions of all three types of collectors to catch a glimpse of the general thermal performances of these collectors and the improvements achievable with the use of the cross-corrugated wavelike absorbing and bottom plates with respect to the flat absorbing plate and bottom plate. A comprehensive parametric study are then followed to examine thermal performances of these three types of collectors under various configurations and operating conditions.

3.1. Results under typical configurations and operating conditions

The following values are used for the parameters under the typical configurations and operating conditions: $I = 600 \text{ W/m}^2$, $\theta = 45^\circ$, $W = 1 \text{ m}$, $L = 2 \text{ m}$, $H_g = 0.05 \text{ m}$, $H_c = 0.05 \text{ m}$, $\dot{m}_f = 0.05 \text{ kg/m}^2 \text{ s}$, $T_a = 300 \text{ K}$, $T_{fi} = 300 \text{ K}$, $\Delta_i = 0.05 \text{ m}$, $k_i = 0.025 \text{ W/m K}$, $\epsilon_{ap} = 0.94$, $\epsilon_{bp} = 0.94$, $\epsilon_c = 0.9$, $\alpha_{ap} = 0.95$, $\alpha_c = 0.06$, $\tau_c = 0.84$, and $h_w = 11.4 \text{ W/m}^2 \text{ K}$.

The results for the typical configurations and operating conditions are listed in Table 1. It is found that the Type 1 and Type 2 collectors, which have the cross-corrugated wavelike absorbing plate and bottom plate, are apparently significantly superior to the Type 3 collector which has the flat absorbing plate and bottom plate, with the efficiencies about 16% higher, indicating that the use of the cross-corrugated wavelike absorbing plate and bottom plate does significantly improve the thermal performance of a solar air collector. Apparently this

improvement of thermal performance is due to the enhanced heat transfer rate inside the air flow channel in the Type 1 and Type 2 collectors, which is about 3.35 times of that in the Type 3 collector, resulting in smaller cover, absorbing plate, and bottom temperatures, and larger heat gains for the fluid in the Type 1 and Type 2 collectors. Although the Type 1 collector has the similar thermal performance to the Type 2 collector, it is found that the latter performs slightly superior to the former. In fact, as will be shown subsequently, these conclusions are also correct under all the configurations and operating conditions considered in this paper.

3.2. Results under various configurations

Although the configuration parameters are W , L , H_g , H_c , Δ_i , k_i , α_{ap} , ϵ_{ap} , ϵ_{bp} , ϵ_c , α_c , and τ_c , it is obvious that small values of α_c and k_i and large values of Δ_i and α_{ap} will result in higher collector efficiencies for all three types of collectors. Further, it is unnecessary to analyze both the effects of L and W . Therefore, only the results for the configuration parameters W , H_g , ϵ_{ap} , ϵ_{bp} , and ϵ_c are presented here to show their effects on the thermal performance of the collectors.

3.2.1. Effect of W and H_g

The results showing the effect of the collector width W on the thermal performance of the three types of collectors are presented in Fig. 1, where W changes in the range of 0.25–5 m, and the values used in the typical configurations and operating conditions as presented in Section 3.1 are used for the other parameters.

From the results, it is found, as observed before, that the Type 1 and Type 2 collectors have much higher efficiencies than the flat-plate solar air collector and the Type 2 collector performs marginally superior to the Type 1 collector for all the values of W considered. With the increase of W , it is found that the efficiencies of all three types of collectors decrease monotonically while the temperatures on the cover, absorbing plate and bottom plate increase monotonically. These trends are mainly due to the monotonic reduce of the convection heat transfer from the absorbing plate to the fluid and the monotonic increases of the thermal radiation heat losses from the absorbing plate to the bottom plate and to the cover when W increases. It is therefore essential to construct a solar air collector which has a slender configuration along the air flow direction (that is, $L > W$) in order to achieve a higher collector efficiency, no matter it is a solar air collector with the cross-corrugated wavelike absorbing plate and bottom plate or one with flat absorbing plate and bottom plate. These observations and conclusions obtained for W were also found true for H_g , the mean gap thickness between the absorbing plate and the bottom plate.

Table 1
Results for the typical configurations and operating conditions

Parameter	Type 1	Type 2	Type 3
η	0.5592	0.5704	0.4021
$q_u \text{ (W/m}^2\text{)}$	335.52	342.27	241.26
$T_c \text{ (K)}$	305.42	305.02	310.39
$T_{ap} \text{ (K)}$	322.23	322.67	339.11
$T_{bp} \text{ (K)}$	309.11	309.31	324.95
$T_{fo} \text{ (K)}$	306.71	306.85	304.83
$h_{r,c-s} \text{ (W/m}^2 \text{ K)}$	18.21	19.19	12.34
$h_{r,ap-c} \text{ (W/m}^2 \text{ K)}$	5.97	5.97	6.62
$h_{c,ap-c} \text{ (W/m}^2 \text{ K)}$	1.43	0.69	0.71
$h_{r,ap-bp} \text{ (W/m}^2 \text{ K)}$	6.33	6.35	7.37
$h_{c,ap-f} \text{ (W/m}^2 \text{ K)}$	13.62	13.62	4.07
Ra	159333	169197	232154
Re	5116	5115	5128
Nu_c	4.98	2.40	2.41
Nu_f	48.95	48.95	14.68

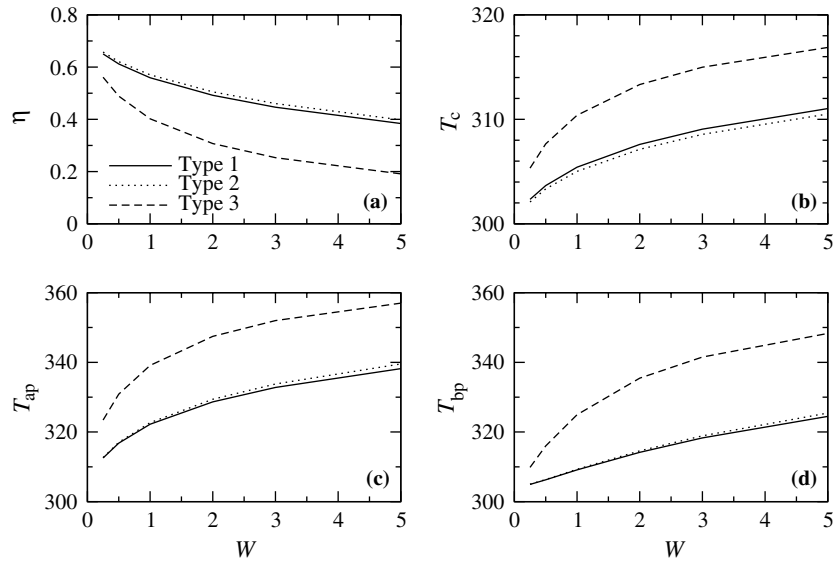


Fig. 1. Effect of W on the thermal performance of three types of solar air collectors with W in the range of 0.25–5 m: (a) η plotted against W , (b) T_c plotted against W , (c) T_{ap} plotted against W , and (d) T_{bp} plotted against W .

3.2.2. Effect of ϵ_{ap} and ϵ_c

The results showing the effect of ϵ_{ap} , the emissivity of thermal radiation of the absorbing plate on the thermal performance of the three types of collectors are presented in Fig. 2, where ϵ_{ap} changes in the range of 0.05–0.94, and the values used in the typical configurations and operating conditions in Section 3.1 are used for the other parameters.

From the results, it is found, once more, that the Type 1 and Type 2 collectors have much higher efficiencies than the flat-plate one and the Type 2 collector performs marginally superior to the Type 1 collector for all the values of ϵ_{ap} considered.

With the increase of ϵ_{ap} , it is found that the efficiencies and the temperature on the absorbing plate of all three types of collectors, as expected, decrease monotonically but at a small rate, while the temperatures on the cover and the bottom plate increase monotonically. The reason for these trends are apparently due to the linear increases of the thermal radiation heat losses from the absorbing plate to the bottom plate and to the cover whereas ϵ_{ap} has little impact on the convection heat transfers from the absorbing plate to the fluid and to the cover. It is therefore essential to main-

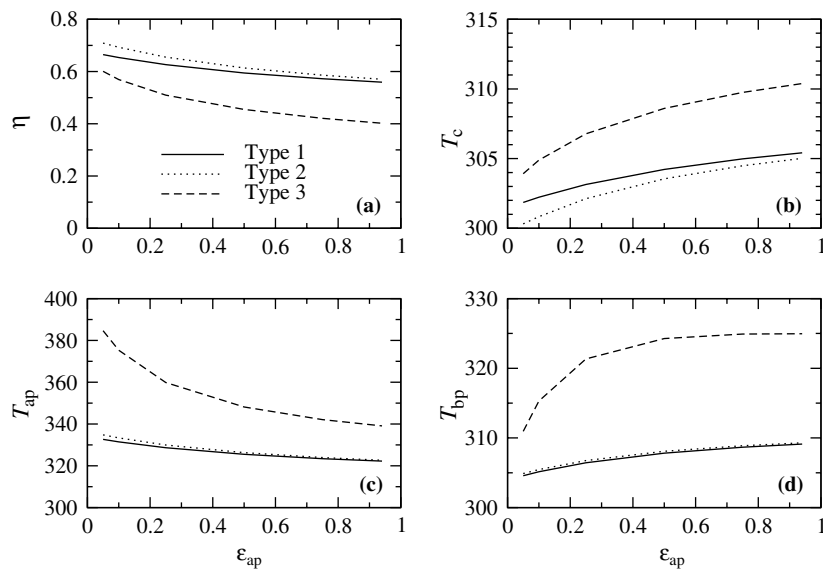


Fig. 2. Effect of ϵ_{ap} with ϵ_{ap} in the range of 0.05–0.94: (a) η plotted against ϵ_{ap} , (b) T_c plotted against ϵ_{ap} , (c) T_{ap} plotted against ϵ_{ap} , and (d) T_{bp} plotted against ϵ_{ap} .

tain the emissivity of thermal radiation on the absorbing plate as small as possible (that is to use a selected coating which has a very high absorptivity of solar radiation but a quite small emissivity of thermal radiation) to achieve a higher collector efficiency, again no matter it is a solar air collector with the cross-corrugated wavelike absorbing plate and bottom plate or one with flat absorbing plate and bottom plate. These observations and conclusions obtained for ϵ_{ap} were also found correct for ϵ_c .

3.2.3. Effect of ϵ_{bp}

The results showing the effect of ϵ_{bp} , the emissivity of thermal radiation of the bottom plate on the thermal performance of the three types of collectors are presented in Fig. 3, where ϵ_{ap} changes in the range of 0.05–0.94, and the values used in the typical configurations and operating conditions in Section 3.1 are used for the other parameters.

From the results, it is confirmed again that the general conclusion obtained above, that is the Type 1 and Type 2 collectors have much higher efficiencies than the flat-plate solar air collector and the Type 2 collector performs marginally superior to the Type 1 collector, is also valid for all the values of ϵ_{bp} considered. The results also show that ϵ_{bp} has little effect on the efficiencies and the temperatures on the absorbing plate and on the cover for all three types of collectors. The temperatures on the bottom plate increase monotonically but slightly with the increase of ϵ_{bp} , as expected. It is further found that the increase of ϵ_{bp} results in a linear increases of the thermal radiation heat losses from the absorbing plate to the bottom plate and from the cover to the sky while

ϵ_{bp} has little impact on the convection heat transfers from the absorbing plate to the fluid and to the cover as well as the thermal radiation heat loss from the absorbing plate to the cover.

3.3. Results under various operating conditions

As mentioned above, the parameters characterizing the operating conditions of the collectors are I , θ , \dot{m}_f , and T_{fi} , respectively. It was found that θ has negligible effect on the thermal performance of all three types of collector. Hence, only the results for the parameters I , \dot{m}_f , and T_{fi} are presented here to show their effects on the thermal performance of the collectors.

3.3.1. Effect of I

The results showing the effect of the solar insolation rate incident on the glass cover I on the thermal performance of the three types of collectors are presented in Fig. 4, where I changes in the range of 100–1000 W/m², and the values used in the typical configurations and operating conditions in Section 3.1 are used for the other parameters.

From the results, it is found again that the Type 1 and Type 2 collectors have much higher efficiencies than the flat-plate solar air collector and the Type 2 collector performs marginally superior to the Type 1 collector for all the values of I considered. The results also show that I has little effect on the efficiencies of all three types of collectors, although the temperatures on the cover, absorbing plate and bottom plate as well as the fluid temperature difference in the air flow channel increase almost linearly with I . The increase of I is observed to

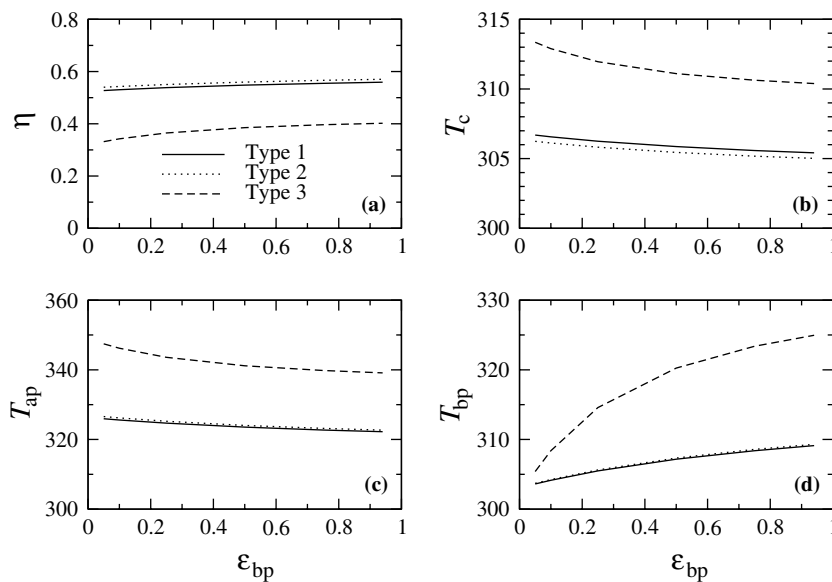


Fig. 3. Effect of ϵ_{bp} with ϵ_{bp} in the range of 0.05–0.94: (a) η plotted against ϵ_{bp} , (b) T_c plotted against ϵ_{bp} , (c) T_{ap} plotted against ϵ_{bp} , and (d) T_{bp} plotted against ϵ_{bp} .

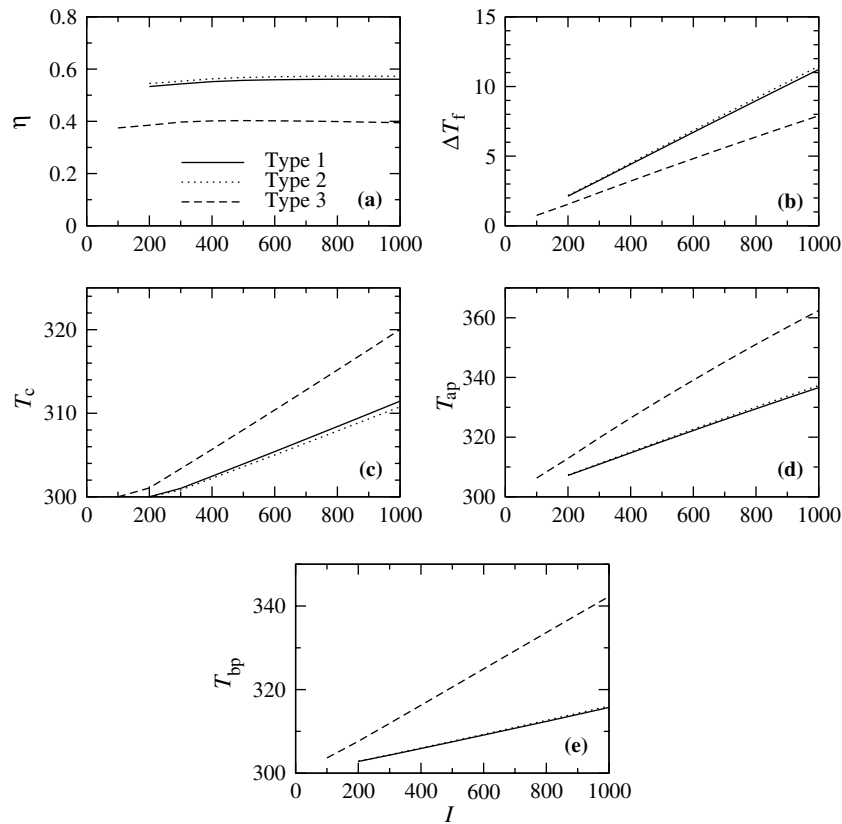


Fig. 4. Effect of I with I in the range of 100–1000 W/m^2 : (a) η plotted against I , (b) ΔT_f plotted against I , where $\Delta T_f = T_{fo} - T_{fi}$, (c) T_c plotted against I , (d) T_{ap} plotted against I , and (e) T_{bp} plotted against I .

linearly increase the thermal radiation heat losses from the absorbing plate to the bottom plate and to the cover but to monotonically reduced the thermal radiation heat loss from the cover to the sky. However, I has no effect on the convection heat transfer between the absorbing plate and the fluid and a marginal effect on the convection heat transfer between the absorbing plate and the cover.

3.3.2. Effect of \dot{m}_f

The results showing the effect of the air mass flow rate per unit area of collector \dot{m}_f on the thermal performance of the three types of collectors are presented in Fig. 5, where \dot{m}_f changes in the range of 0.001–0.25 $\text{kg/m}^2 \text{s}$, and the values used in the typical configurations and operating conditions in Section 3.1 are used for the other parameters.

From the results, it is found once more that the Type 1 and Type 2 collectors have much higher efficiencies than the flat-plate solar air collector and the Type 2 collector performs marginally superior to the Type 1 collector for all the values of \dot{m}_f considered. The results also show that the efficiencies of all three types of collectors increase monotonically and dramatically with \dot{m}_f , although the temperatures on the cover, absorbing plate and bottom plate as well as the fluid temperature differ-

ence in the air flow channel decrease monotonically. The increase of \dot{m}_f is observed to dramatically enhance the convection heat transfer from the absorbing plate to the fluid, especially for the Type 1 and Type 2 collectors, while at the same time to reduce monotonically the convection heat transfer from the absorbing plate to the cover and the thermal radiation heat losses from the absorbing plate to both the bottom plate and the cover. It is also observed that the increase of \dot{m}_f significantly increases the thermal radiation heat loss from the cover to the sky for the Type 1 and Type 2 collector while for the flat-plate collector this increase is at a much smaller rate. Therefore, it is essential to maintain a higher air mass flow rate to achieve a better thermal performance of the collectors.

3.3.3. Effect of T_{fi}

The results showing the effect of the inlet fluid temperature T_{fi} on the thermal performance of the three types of collectors are presented in Fig. 6, where T_{fi} changes in the range of 280–360 K, and the values used in the typical configurations and operating conditions in Section 3.1 are used for the other parameters.

From the results, it is confirmed again that the Type 1 and Type 2 collectors have much higher efficiencies than the flat-plate solar air collector and the Type 2 collector

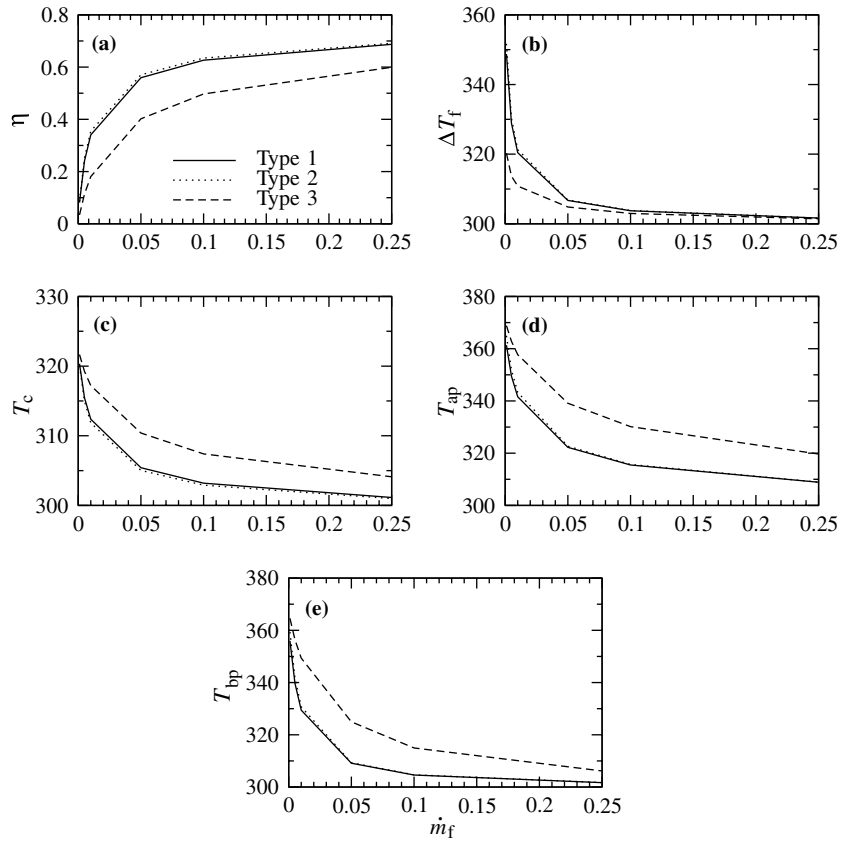


Fig. 5. Effect of \dot{m}_f with \dot{m}_f in the range of 0.001–0.25 kg/m² s: (a) η plotted against \dot{m}_f , (b) ΔT_f plotted against \dot{m}_f , (c) T_c plotted against \dot{m}_f , (d) T_{ap} plotted against \dot{m}_f , and (e) T_{bp} plotted against \dot{m}_f .

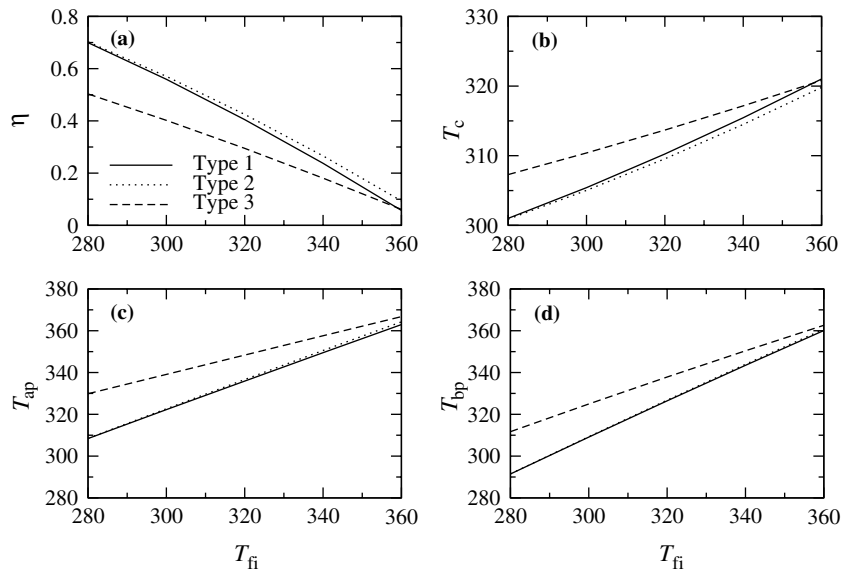


Fig. 6. Effect of T_{fi} with T_{fi} in the range of 280–360 K: (a) η plotted against T_{fi} , (b) T_c plotted against T_{fi} , (c) T_{ap} plotted against T_{fi} , and (d) T_{bp} plotted against T_{fi} .

performs marginally superior to the Type 1 collector for all the values of T_{fi} considered. The results show that the efficiencies of all three types of collectors decrease dra-

matically and almost linearly with T_{fi} , while the temperatures on the cover, absorbing plate and bottom plate increase significantly and also almost linearly with T_{fi} .

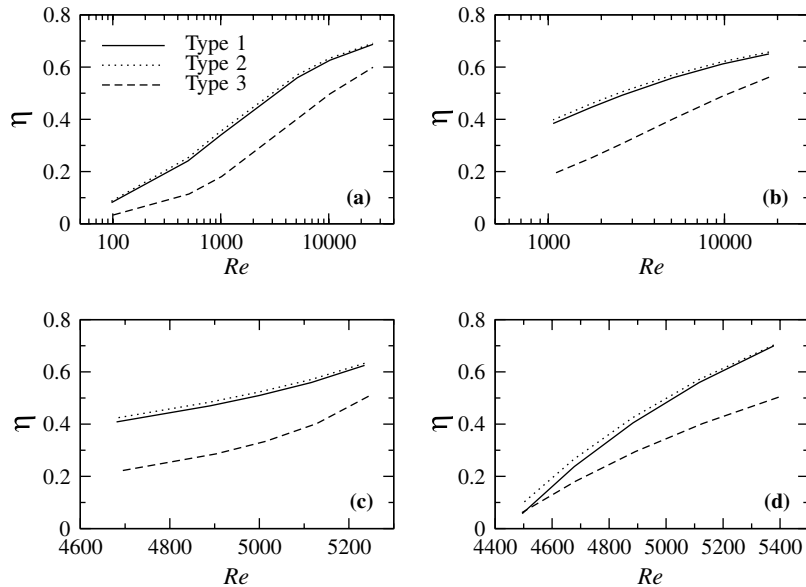


Fig. 7. Effect of Re : (a) with the \dot{m}_f variation, (b) with the W variation, (c) with the H_g variation, and (d) with the T_{fi} variation.

However, T_{fi} has little effect on the convection heat transfer from the absorbing plate to the fluid for all three types of collectors and those from the absorbing plate to the cover for the Type 2 collector and the flat-plate collector while it increases the convection heat transfer between the absorbing plate to the cover for the Type 1 collector. It is further observed that T_{fi} increases the thermal radiation heat losses from the absorbing plate to both the bottom plate and the cover but reduces that from the cover to the sky. Therefore, it is essential to maintain the inlet fluid temperature close to that of the ambient fluid to achieve a better thermal performance of the collectors.

3.4. Effect of Re on overall collector performance

It is of interest to know the effect of the Reynolds number Re on the overall performance of these three types of air collectors. Such effects are depicted in Fig. 7 where the efficiencies of all three collectors are plotted against Re with the \dot{m}_f variation, the W variation, the H_g variation, and the T_{fi} variation, respectively. The results show that the efficiencies of all three collectors increase with Re for all variations considered, although the variations of \dot{m}_f and W result in very large ranges of Re whereas the variations of H_g and T_{fi} result in quite small ranges of Re . It is further observed that the two types of cross-corrugated solar air collectors have a significantly superior thermal performance to that of the flat-plate one, which is in line with the above observations. An increase of Re will enhance the convection heat transfer inside the air channel which will in turn augment the overall collector performance.

As Re is determined by the mass flow rate, the air property, and the air channel configuration, it is

expected that all parameters except \dot{m}_f , W , H_g and T_{fi} , that is the parameters such as I , θ , ϵ_{ap} , ϵ_{bp} , etc., have little effect on Re which are confirmed by the analytical results.

4. Conclusions

A comprehensive parametric study has been carried out on the thermal performance of cross-corrugated solar air collectors under various configurations and operating conditions. These collectors consist of a wavelike absorbing plate and a wavelike bottom plate which are crosswise positioned to form the air flow channel, with the aim to enhance the turbulence and heat transfer rate inside the air flow channel which are crucial to the improvement of efficiencies of solar air collectors. Two types of these collectors are considered. For the Type 1 collector, the wavelike shape of the absorbing plate is along the flow direction and that of the bottom plate is perpendicular to the flow direction, while for the Type 2 collector it is the wavelike shape of the bottom plate that is along the flow direction and that of the absorbing plate is perpendicular to the flow direction. To quantify the achievable improvements with the cross-corrugated absorbing and bottom plates, a flat-plate solar air collector which has both a flat absorbing plate and a flat bottom plate, is also considered. The results can be summarized as follows:

- (1) Although the thermal performance of the Type 2 collector is just slightly superior to that of the Type 1 collector, both these cross-corrugated solar air collectors have a significantly superior thermal performance to that of the flat-plate one, with

the achievable efficiencies of 55.92%, 57.04% and 40.21% for the Type 1, Type 2 and flat-plate solar air collectors, respectively, under the typical configurations and operating conditions.

- (2) To achieve a higher collector efficiency, it is essential to construct solar air collectors having slender configurations along the air flow direction, to maintain a small gap between the absorbing plate and bottom plate, to use selected coatings which have very high absorptivities of solar radiation but very small emissivities of thermal radiation on the absorbing plate and glass cover, to maintain a higher air mass flow rate, and to operate the collectors with the inlet fluid temperature close to that of the ambient fluid, no matter it is a collector with the cross-corrugated wavelike absorbing plate and bottom plate or one with flat absorbing plate and bottom plate.
- (3) The solar insolation rate incident on the collectors, the inclination of the collectors, and the emissivity of thermal radiation on the bottom plate have negligible effects on the efficiencies of the collectors although they may have significant effects on the temperatures on the cover, absorbing plate, and bottom plate, and on the heat transfer rate between various plates and the fluid.

Acknowledgements

The financial support from the National Natural Science Foundation of China (Grant No. 10262003), the Natural Science Foundation of Yunnan Province (Key Projects, Grant No. 2003E0004Z), The International Collaboration Scheme of Yunnan Province, and the Program for New Century Excellent Talents in University of China (Grant No. NCET-04-0918) are gratefully acknowledged.

References

- [1] J.A. Duffie, W.A. Beckman, *Solar Engineering of Thermal Processes*, second ed., John Wiley & Sons, New York, 1991.
- [2] W.C. Dickson, P.N. Cheremisinoff, *Solar Energy Technology Handbook*, Marcel Dekker, USA, 1980.
- [3] J.R. Williams, *Design and Installation of Solar Heating and Hot Water Systems*, Ann Arbor Science Publishers, New York, 1983.
- [4] L. Goldstein, E.M. Sparrow, Experiments on the transfer characteristics of a corrugated fin and tube heat exchanger configuration, *Transaction of the ASME, Journal of Heat Transfer* 98 (1976) 26–34.
- [5] L. Goldstein, E.M. Sparrow, Heat/mass transfer characteristics for flow in a corrugated wall channel, *Transaction of the ASME, Journal of Heat Transfer* 99 (1977) 187–195.
- [6] B.A. Meyer, J.W. Mitchell, M.M. El-Wakil, Convective heat transfer in Vee-trough linear concentrators, *Solar Energy* 28 (1982) 33–40.
- [7] X.W. Zhao, Z.N. Li, Numerical and experimental study on free convection in air layers with one surface V-corrugated, in: *Proceedings of the Annual Meeting of the Chinese Society of Solar Energy* in 1991, 1991, pp. 182–192.
- [8] J.A. Stasiek, Experimental studies of heat transfer and fluid flow across corrugated-undulated heat exchanger surfaces, *International Journal of Heat and Mass Transfer* 41 (1998) 899–914.
- [9] Y. Piao, E.G. Hauptmann, M. Iqbal, Forced convective heat transfer in cross-corrugated solar air heaters, *Transactions of the ASME, Journal of Solar Energy Engineering* 116 (1994) 212–214.
- [10] Y. Piao, Natural, forced and mixed convection in a vertical cross corrugated channel, M.Sc. Thesis, The University of British Columbia, Canada, 1992.
- [11] S. Noorshahi, C.A. Hall III, E.K. Glakpe, Natural convection in a corrugated enclosure with mixed boundary conditions, *Transaction of the ASME, Journal of Solar Energy Engineering* 118 (1996) 50–57.
- [12] W.F. Gao, Analysis and performance of a solar air heater with cross corrugated absorber and back-plate, M.Sc. Thesis, Yunnan Normal University, China, 1996.
- [13] W.F. Gao, W.X. Lin, E. Lu, Numerical study on natural convection inside the channel between the flat-plate cover and sine-wave absorber of a cross-corrugated solar air heater, *Energy Conversion and Management* 41 (2000) 145–151.
- [14] W.H. McAdams, *Heat Transmission*, third ed., McGraw-Hill, New York, 1954.
- [15] X.Q. Zhai, Y.J. Dai, R.Z. Wang, Comparison of heating and natural ventilation in a solar house induced by two roof solar collectors, *Applied Thermal Engineering* 25 (2005) 741–757.
- [16] W.C. Swinbank, Long-wave radiation from clear skies, *Quarterly Journal of the Royal Meteorological Society* 89 (1963) 339.
- [17] K.G.T. Hollands, T.E. Unny, G.D. Raithby, L.J. Konicek, Free convection heat transfer across inclined air layers, *Transactions of the ASME, Journal of Heat Transfer* 98 (1976) 189–193.
- [18] W.M. Kays, M.E. Crawford, *Convective Heat and Mass Transfer*, second ed., McGraw-Hill, New York, 1980.
- [19] R.C. Weast (Ed.), *Handbook of Tables for Applied Engineering Science*, CRC Press, Boca Raton, FA, 1970.